10442 *Inorg. Chem.* **2009**, *48*, 10442–10454
DOI: 10.1021/ic901524s

Inorganic Chemistry
Article

Sulfonamide-Supported Group 4 Catalysts for the Ring-Opening Polymerization of ε-Caprolactone and *rac*-Lactide

Andrew D. Schwarz, Amber L. Thompson, and Philip Mountford*

Chemistry Research Laboratory, University of Oxford, Mansfield Road, Oxford OX1 3TA, U.K.

Received July 31, 2009

Reaction of $RCH_2N(CH_2CH_2NHSO_2Tol)_2$ (R=2-NC_5H_4 (**8**, H_2L^{py}) or $MeOCH_2$ (**9**, H_2L^{OMe})) with $Ti(NMe_2)_4$ at room temperature afforded $Ti(L^{py})(NMe_2)_2$ (**10**) or $Ti(L^{OMe})(NMe_2)_2$ (**11**), respectively, which contain tetradentate bis(sulfonamide)amine ligands. The corresponding reactions with $Ti(O^iPr)_4$ or $Zr(O^iPr)_4 \cdot HO^iPr$ required more forcing conditions to form the homologous bis(isopropoxide) analogues, $M(L^R)(O^iPr)_2$ (M=Ti, R=py (**12**) or OMe (**14**); M=Zr, R=py (**13**) or OMe (**15**)). Reaction of $Ti(NMe_2)_2(O^iPr)_2$ with H_2L^R formed **12** or **14** under milder conditions. The X-ray structures of **10**−**15** have been determined revealing C_s symmetric, 6-coordinate complexes except for **13** which is 7-coordinate with one $\kappa^2(N,O)$ bound sulfonamide donor. Compounds **10**− **15** are all catalysts for the ring-opening polymerization (ROP) of ε-caprolactone, with the isopropoxide compounds being the fastest and best controlled, especially in the case of zirconium. In addition, $Zr(L^{OMe})(O^iPr)_2$ (**15**) was an efficient catalyst for the well-controlled ROP of *rac*-lactide both in toluene at 100 °C and in the melt at 130 °C, giving atactic poly(*rac*-lactide). The polymerization rates and control achieved for **13** and **15** are comparable to those of the well-established bis(phenolate)amine-supported Group 4 systems reported recently.

Introduction

There is much current interest in the controlled ring-opening polymerization (ROP) of cyclic esters such as ε-caprolactone (ε-CL) and *rac*-lactide (*rac*-LA) because of the biocompatibility and biodegradability of the resulting polyesters. These polymers can act as replacements for oil-based materials and can be derived from 100% renewable resources including corn and sugar beet.[1−7] Metal-based catalysts for the ROP of cyclic esters have been extensively reviewed.[8−11] They can be derived from a variety of Lewis acids, typically magnesium,[12−15] zinc,[12,14,16−19] calcium,[15,20,21] aluminum,[19,22−25] yttrium,[26,27] the lanthanides,[28−30] tin,[31] Group 4 elements,[19,32−38] and iron.[39,40] They generally feature one or more alkoxide functional (initiating) groups, and are supported by a polydentate ancillary ligand which effects control of the catalyst nuclearity and coordination−insertion chain growth mechanism.

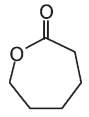

ε-caprolactone (ε-CL)

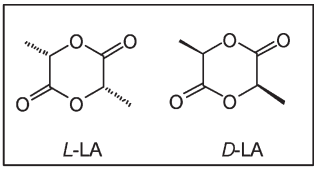

rac-lactide (*rac*-LA)

Among the transition metals, Group 4 complexes have exhibited very good control of the polymerization process,

*To whom correspondence should be addressed. E-mail: philip.mountford@chem.ox.ac.uk.

(1) Emo, C.; Roberto, S. *Adv. Mater.* **1996**, *8*, 305–313.
(2) Uhrich, K. E.; Cannizzaro, S. M.; Langer, R. S.; Shakesheff, K. M. *Chem. Rev.* **1999**, *99*, 3181–3198.
(3) Drumright, R. E.; Gruber, P. R.; Henton, D. E. *Adv. Mater.* **2000**, *12*, 1841–1846.
(4) Yoshito, I.; Hideto, T. *Macromol. Rapid Commun.* **2000**, *21*, 117–132.
(5) Stefan, M. *Angew. Chem., Int. Ed.* **2004**, *43*, 1078–1085.
(6) Williams, C. K.; Hillmyer, M. A. *Polym. Rev.* **2008**, *48*, 1–10.
(7) Place, E. S.; George, J. H.; Williams, C. K.; Stevens, M. M. *Chem. Soc. Rev.* **2009**, *38*, 1139–1151.
(8) Dechy-Cabaret, O.; Martin-Vaca, B.; Bourissou, D. *Chem. Rev.* **2004**, *104*, 6147–6176.
(9) O'Keefe, B. J.; Hillmyer, M. A.; Tolman, W. B. *J. Chem. Soc., Dalton Trans.* **2001**, 2215–2224.
(10) Platel, R. H.; Hodgson, L. M.; Williams, C. K. *Polym. Rev.* **2008**, *48*, 11–63.
(11) Kamber, N. E.; Jeong, W.; Waymouth, R. M.; Pratt, R. C.; Lohmeijer, B. G. G.; Hedrick, J. L. *Chem. Rev.* **2007**, *107*, 5813–5840.
(12) Chamberlain, B. M.; Cheng, M.; Moore, D. R.; Ovitt, T. M.; Lobkovsky, E. B.; Coates, G. W. *J. Am. Chem. Soc.* **2001**, *123*, 3229–3238.
(13) Chisholm, M. H.; Eilerts, N. W. *Chem. Commun.* **1996**, 853–854.
(14) Chisholm, M. H.; Huffman, J. C.; Phomphrai, K. *J. Chem. Soc., Dalton Trans.* **2001**, 222–224.
(15) Wheaton, C. A.; Hayes, P. G.; Ireland, B. J. *Dalton Trans.* **2009**, 4832–4846.
(16) Cheng, M.; Attygalle, A. B.; Lobkovsky, E. B.; Coates, G. W. *J. Am. Chem. Soc.* **1999**, *121*, 11583–11584.
(17) Chisholm, M. H.; Eilerts, N. W.; Huffman, J. C.; Iyer, S. S.; Pacold, M.; Phomphrai, K. *J. Am. Chem. Soc.* **2000**, *122*, 11845–11854.
(18) Wheaton, C. A.; Ireland, B. J.; Hayes, P. G. *Organometallics* **2009**, *28*, 1282–1285.

Published on Web 09/28/2009

featuring reasonably fast initiation and minimal side reactions (chain transfer). This leads to polymers of well-defined and predictable molecular weights (M_n), narrow polydispersity indices (PDIs), and (for *rac*-LA) heterotactic enrichment.[32,41,42] Early work[32] with these metals was based around simple homoleptic metal alkoxides $M(OR)_4$ (R = alkyl; M = Ti or Zr),[32,43] which operate as ROP catalysts via a coordination−insertion mechanism. Aida et al. employed bidentate bis(phenolate) ancillary ligands on titanium with isopropoxide initiating groups, obtaining poly(ε-CL) with narrow PDI (ca. 1.2) (**1** in Figure 1).[44,45] Subsequent work by Verkade et al. employed titanatranes of various structures featuring either bulky aryloxide or isopropoxide initiating groups.[33,46−48] Concurrent with these developments, Harada et al. reported bulky bidentate and tridentate phenolate complexes of titanium bearing isopropoxide and diethylamido initiator groups. These species demonstrated moderate activities and control for polymerization of ε-CL and LA in toluene at elevated temperatures.[49,50] Gibson and Long used aminophenoxide ligands bound to titanium for the polymerization of LA in toluene at 70 °C and obtained poly(LA) of narrow PDI (1.1−1.2) with good activity (e.g., 96% conversion after 6 h). However, where *rac*-LA was employed, no significant control over polymer tacticity was obtained.[51,52] Interestingly, upon employing complex **2** (Figure 1) it was possible to moderate catalyst activity by redox control of the ferrocenyl groups on the ligand periphery.[53] Significant advances have been achieved recently using tetradentate bis(phenolate)diamine and related ancillary ligands such as in **3** and **4** (Figure 1).[41,42,54−57] Good control has also been achieved for the ROP of *rac*-LA under industrially desirable melt conditions. C_3-symmetric zirconium tris(phenolate)-amine isopropoxide complexes of the type **4** (Figure 1) act as well-controlled single site catalysts that give both narrow PDIs and highly heterotactically enriched poly(*rac*-LA).[54]

We have recently been interested to develop new supporting ligands for Group 4 ROP catalysts and speculated that polydentate sulfonamides (containing $-N(R)SO_2R'$ functional groups) could be useful in this regard. The electron-withdrawing SO_2R' moieties reduce the normal basicity of anionic amide donors "NR_2" and might therefore allow them to act as phenolate mimics. Although $N(R)SO_2R'$ based ligands lack the steric control afforded by bulky ring-substituted phenolates OAr (e.g., **3** and **4** in Figure 1), the well-established ability of sulfonamide ligands to adopt $\kappa^2(N,O)$ coordination modes[58−68] could confer additional stability on

(19) Chisholm, M. H.; Lin, C.-C.; Gallucci, J. C.; Ko, B.-T. *Dalton Trans.* **2003**, 406–412.
(20) Zhong, Z.; Dijkstra, P. J.; Birg, C.; Westerhausen, M.; Feijen, J. *Macromolecules* **2001**, *34*, 3863–3868.
(21) Antelmann, B.; Chisholm, M. H.; Iyer, S. S.; Huffman, J. C.; Navarro-Llobet, D.; Pagel, M.; Simonsick, W. J.; Zhong, W. *Macromolecules* **2001**, *34*, 3159–3175.
(22) Dubois, P.; Jerome, R.; Teyssie, P. *Macromolecules* **1991**, *24*, 977–981.
(23) Kowalski, A.; Duda, A.; Penczek, S. *Macromolecules* **1998**, *31*, 2114–2122.
(24) Aida, T.; Inoue, S. *Acc. Chem. Res.* **1996**, *29*, 39–48.
(25) Cameron, P. A.; Jhurry, D.; Gibson, V. C.; White, A. J. P.; Williams, D. J.; Williams, S. *Macromol. Rapid Commun.* **1999**, *20*, 616–618.
(26) McLain, S. J.; Ford, T. M.; Drysdale, N. E. *Polym. Prepr.* (*Am. Chem. Soc., Div. Polym. Chem.*) **1992**, *33*, 463.
(27) Chamberlain, B. M.; Sun, Y.; Hagadorn, J. R.; Hemmesch, E. W.; Young, V. G., Jr; Hillmyer, M. A.; Tolman, W. B. *Macromolecules* **1999**, *32*, 2400–2402.
(28) Giesbrecht, G. R.; Whitener, G. D.; Arnold, J. *J. Chem. Soc., Dalton Trans.* **2001**, 923–927.
(29) Dyer, H. E.; Huijser, S.; Schwarz, A. D.; Wang, C.; Duchateau, R.; Mountford, P. *Dalton Trans.* **2008**, 32–35.
(30) Bonnet, F.; Cowley, A. R.; Mountford, P. *Inorg. Chem.* **2005**, *44*, 9046–9055.
(31) Kricheldorf, H. R.; Kreiser-Saunders, I.; Boettcher, C. *Polymer* **1995**, *36*, 1253–1259.
(32) Kricheldorf, H. R.; Berl, M.; Scharnagl, N. *Macromolecules* **1988**, *21*, 286–293.
(33) Kim, Y.; Jnaneshwara, G. K.; Verkade, J. G. *Inorg. Chem.* **2003**, *42*, 1437–1447.
(34) Thomas, D.; Arndt, P.; Peulecke, N.; Spannenberg, A.; Kempe, R.; Rosenthal, U. *Eur. J. Inorg. Chem.* **1998**, *1998*, 1351–1357.
(35) Dobrzynski, P.; Li, S.; Kasperczyk, J.; Bero, M.; Gasc, F.; Vert, M. *Biomacromolecules* **2005**, *6*, 483–488.
(36) Mogstad, A.-L.; Waymouth, R. M. *Macromolecules* **1994**, *27*, 2313–2315.
(37) Miola Delaite, C.; Hamaide, T.; Spitz, R. *Macromol. Chem. Phys.* **1999**, *200*, 1771–1778.
(38) Hsieh, K. C.; Lee, W. Y.; Hsueh, L. F.; Lee, H. M.; Huang, J. H. *Eur. J. Inorg. Chem.* **2006**, 2306–2312.
(39) O'Keefe, B. J.; Monnier, S. M.; Hillmyer, M. A.; Tolman, W. B. *J. Am. Chem. Soc.* **2001**, *123*, 339–340.
(40) O'Keefe, B. J.; Breyfogle, L. E.; Hillmyer, M. A.; Tolman, W. B. *J. Am. Chem. Soc.* **2002**, *124*, 4384–4393.
(41) Gendler, S.; Segal, S.; Goldberg, I.; Goldschmidt, Z.; Kol, M. *Inorg. Chem.* **2006**, *45*, 4783–4790.
(42) Chmura, A. J.; Davidson, M. G.; Jones, M. D.; Lunn, M. D.; Mahon, M. F. *Dalton Trans.* **2006**, 887–889.
(43) Cayuela, J.; Bounor-Legare, V.; Cassagnau, P.; Michel, A. *Macromolecules* **2006**, *39*, 1338–1346.
(44) Takeuchi, D.; Nakamura, T.; Aida, T. *Macromolecules* **2000**, *33*, 725–729.
(45) Takeuchi, D.; Aida, T. *Macromolecules* **2000**, *33*, 4607–4609.
(46) Kim, Y.; Verkade, J. G. *Organometallics* **2002**, *21*, 2395–2399.
(47) Youngjo, K.; John, G. V. *Macromol. Rapid Commun.* **2002**, *23*, 917–921.
(48) Youngjo, K.; John, G. V. *Macromol. Symp.* **2005**, *224*, 105–118.
(49) Takashima, Y.; Nakayama, Y.; Watanabe, K.; Itono, T.; Ueyama, N.; Nakamura, A.; Yasuda, H.; Harada, A.; Okuda, J. *Macromolecules* **2002**, *35*, 7538–7544.
(50) Takashima, Y.; Nakayama, Y.; Hirao, T.; Yasuda, H.; Harada, A. *J. Organomet. Chem.* **2004**, *689*, 612–619.
(51) Atkinson, R. C. J.; Gerry, K.; Gibson, V. C.; Long, N. J.; Marshall, E. L.; West, L. J. *Organometallics* **2006**, *26*, 316–320.
(52) Gregson, C. K. A.; Blackmore, I. J.; Gibson, V. C.; Long, N. J.; Marshall, E. L.; White, A. J. P. *Dalton Trans.* **2006**, 3134–3140.
(53) Gregson, C. K. A.; Gibson, V. C.; Long, N. J.; Marshall, E. L.; Oxford, P. J.; White, A. J. P. *J. Am. Chem. Soc.* **2006**, *128*, 7410–7411.
(54) Chmura, A. J.; Davidson, M. G.; Frankis, C. J.; Jones, M. D.; Lunn, M. D. *Chem. Commun.* **2008**, 1293–1295.
(55) Sarazin, Y.; Howard, R. H.; Hughes, D. L.; Humphrey, S. M.; Bochmann, M. *Dalton Trans.* **2006**, 340–350.
(56) Chmura, A. J.; Cousins, D. M.; Davidson, M. G.; Jones, M. D.; Lunn, M. D.; Mahon, M. F. *Dalton Trans.* **2008**, 1437–1443.
(57) Chmura, A. J.; Davidson, M. G.; Jones, M. D.; Lunn, M. D.; Mahon, M. F.; Johnson, A. F.; Khunkamchoo, P.; Roberts, S. L.; Wong, S. S. F. *Macromolecules* **2006**, *39*, 7250–7257.
(58) Armistead, L. T.; White, P. S.; Gagne, M. R. *Organometallics* **1998**, *17*, 216–220.
(59) Armistead, L. T.; White, P. S.; Gagne, M. R. *Organometallics* **1998**, *17*, 4232–4239.
(60) Pritchett, S.; Gantzel, P.; Walsh, P. J. *Organometallics* **1997**, *16*, 5130–5132.
(61) Pritchett, S.; Woodmansee, D. H.; Gantzel, P.; Walsh, P. J. *J. Am. Chem. Soc.* **1998**, *120*, 6423–6424.
(62) Pritchett, S.; Gantzel, P.; Walsh, P. J. *Organometallics* **1999**, *18*, 823–831.
(63) Lensink, C.; Gainsford, G. J.; Baxter, N. I. *Acta Crystallogr., Sect. C: Cryst. Struct, Commun.* **2001**, *57*, 366–367.
(64) Lensink, C.; Gainsford, G. J.; Baxter, N. I. *Acta Crystallogr., Sect. C: Cryst. Struct, Commun.* **2001**, *57*, 368–369.
(65) Hamura, S.; Oda, T.; Shimizu, Y.; Matsubara, K.; Nagashima, H. *J. Chem. Soc., Dalton Trans.* **2002**, 1521–1527.
(66) Ackermann, L.; Bergman, R. G.; Loy, R. N. *J. Am. Chem. Soc.* **2003**, *125*, 11956–11963.
(67) Costa, A. M.; García, C.; Carroll, P. J.; Walsh, P. J. *Tetrahedron* **2005**, *61*, 6442–6446.
(68) Massimiliano, F.; Fredrik, L.; Myriam Mba, B.; Patrick, R.; Marco, C.; Lutz, H. G.; Giulia, L.; Christina, M. *Eur. J. Inorg. Chem.* **2006**, *2006*, 1032–1040.

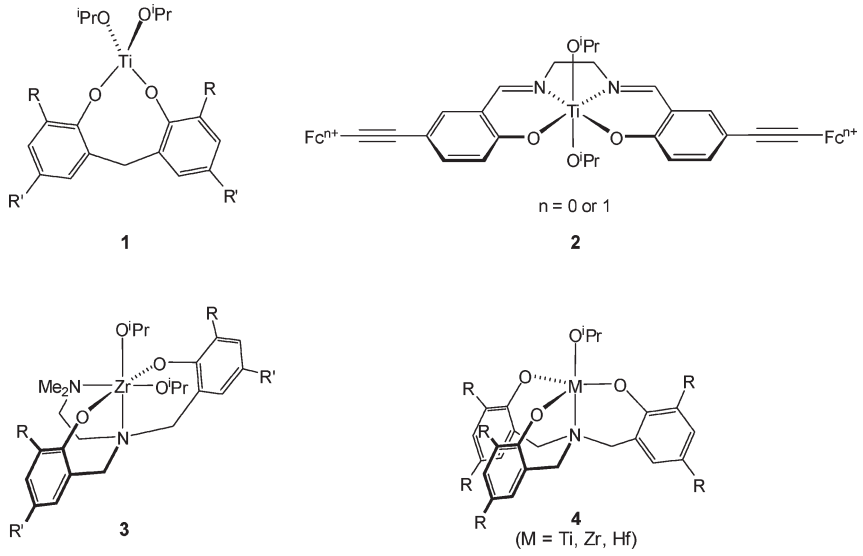

Figure 1. Examples of Group 4 catalysts for the ROP of cyclic esters.[41,42,44,45,53,54]

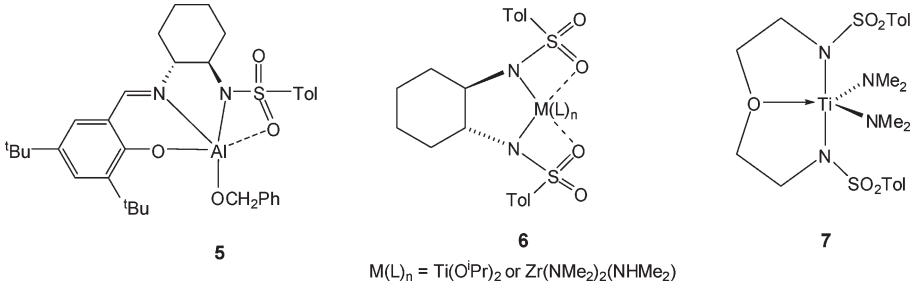

Figure 2. Examples of a recent aluminum ROP catalyst[69] and selected Group 4 sulfonamide compounds.[60,65,66]

otherwise unsaturated metal centers. Sulfonamides in general are attractive synthetic targets because of their relatively simple preparation from the corresponding sulfonyl chlorides, a wide range of which are commercially available. There have been only two reports of sulfonamide-supported ROP catalysts to date, in both cases for aluminum (e.g., complex **5**, Figure 2).[69,70] Although **5** is a very slow catalyst for the ROP of L-lactide, the polymerization was well-controlled suggesting that sulfonamide complexes of Group 4 metals (which show higher intrisic activities compared with aluminum) would be appropriate targets. A number of Group 4 (in particular titanium) complexes of certain bi- and tridentate bis(sulfonamide) ligands have been reported over the past 10 years (see Figure 2 for examples) and are effective for a variety of catalytic transformations such as synthesis of acetylenic alcohols,[71] enantioselective addition of diethyl zinc to benzaldehyde,[62,72] hydroamination of alkynes and allenes,[66] and Zeigler-Natta catalysis.[73] Some selected examples are given in Figure 2.[61,72] To date, no Group 4 sulfonamide compounds have been evaluated as catalysts for ROP.

In this contribution we report the synthesis and structures of a series of new titanium and zirconium complexes derived from the N_4-donor sulfonamide $(2\text{-}NC_5H_4)CH_2N(CH_2CH_2NHSO_2Tol)_2$ (**8**, H_2L^{py}) and the related N_3O-donor $MeOCH_2CH_2N(CH_2CH_2NHSO_2Tol)_2$ (**9**, H_2L^{OMe}) together with their performance as ROP catalysts for ε-CL and *rac*-LA.

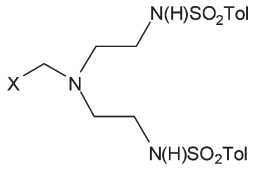

Results and Discussion

Synthesis. The known[74,75] protio-ligands H_2L^{py} (**8**) and H_2L^{OMe} (**9**) were synthesized in high yield by ring-opening reactions of N-tosyl aziridine with the appropriate amine, namely, $2\text{-}NC_5H_4CH_2NH_2$ or $MeOCH_2CH_2NH_2$, respectively. Although the solid state structure of **8** has been previously described, that of **9** has not been

(69) Wu, J.; Pan, X.; Tang, N.; Lin, C.-C. *Eur. Polym. J.* **2007**, *43*, 5040–5046.
(70) Zhao, J.; Song, H.; Cui, C. *Organometallics* **2007**, *26*, 1947–1954.
(71) Lütjens, H.; Nowotny, S.; Knochel, P. *Tetrahedron: Asymmetry* **1995**, *6*, 2675–2678.
(72) Cheng, G.; Jun, Q.; Zhang, X.; Verdugo, D.; Larter, M. L.; Christie, R.; Kenney, P.; Walsh, P. J. *Tetrahedron* **1997**, *53*, 4145–4158.
(73) Padmanabhan, S.; Govindarajan, S. *J. Polym. Sci., Part A: Polym. Chem.* **2006**, *44*, 4006–4014.
(74) Skinner, M. E. G.; Li, Y.; Mountford, P. *Inorg. Chem.* **2002**, *41*, 1110–1119.
(75) Bailey, N. A.; Fenton, D. E.; Hellier, P. C.; Hempstead, P. D.; Casellatob, U.; Vigatob, P. A. *Dalton Trans.* **1992**, 2809–2816.

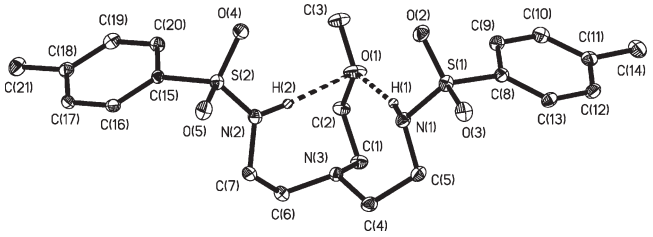

Figure 3. Displacement ellipsoid plot of H_2L^{OMe} (**9**). C-bound H atoms are omitted for clarity, H(1) and H(2) are drawn as spheres of arbitrary radius, and the ellipsoids are drawn at the 20% probability level.

Table 1. Selected Bond Distances (Å) and Angles (deg) for H_2L^{OMe} (**9**)

N(1)−S(1)	1.618(2)	S(2)−O(5)	1.432(2)
N(2)−S(2)	1.602(2)	N(1)−H(1)	0.83(3)
S(1)−O(2)	1.433(2)	N(2)−H(2)	0.92(3)
S(1)−O(3)	1.432(2)	H(1)···O(1)	2.20(4)
S(2)−O(4)	1.434(2)	H(2)···O(1)	2.53(4)
N(1)−H(1)···O(1)	168(3)	S(1)−N(1)−H(1)	106(2)
N(2)−H(2)···O(1)	155(3)	H(1)−N(1)−C(5)	111(2)
C(3)−O(1)−C(2)	112.2(2)	S(2)−N(2)−C(7)	121.3(2)
C(3)−O(1)···H(1)	131.0(9)	S(2)−N(2)−H(2)	120(2)
C(3)−O(1)···H(2)	105.6(8)	H(2)−N(2)−C(7)	115(2)
S(1)−N(1)−C(5)	118.84(18)		

reported. Therefore, for comparison with its metal complexes described below, the X-ray structure of **9** was determined. The molecular structure is shown in Figure 3 and selected distances and angles are listed in Table 1.

Molecules of H_2L^{OMe} possess two intramolecular N−H···O hydrogen bonds between the two sulfonamide nitrogens and the OMe group oxygen atom. This preorganizes **9** into a geometry akin to that required to bind a metal center. All bond lengths and angles for **9** lie within the expected ranges for compounds of this type.[76] Protioligand H_2L^{py} (**8**) also crystallized in a pre-organized manner, but in that case an EtOH molecule of crystallization was incorporated into the ligand cavity through multiple H-bonding interactions.[74]

Protonolysis reactions of **8** or **9** with 1 equiv of $Ti(NMe_2)_4$ in benzene at ambient temperature gave the bis(dimethylamide) complexes $Ti(L^{py})(NMe_2)_2$ (**10**) and $Ti(L^{OMe})(NMe_2)_2$ (**11**), respectively, in 50−55% yield after recrystallization (Scheme 1). When followed in CD_2Cl_2 on the NMR tube scale the yields were effectively quantitative and the expected $HNMe_2$ side product was observed. The solid state structures of both compounds have been determined (vide infra) and confirm those shown in Scheme 1. The solution NMR spectra at 303 K (for **10**) or ambient temperature (for **11**) are also consistent with the C_s symmetric solid state structures. However, cooling the NMR samples of **10** to ambient temperature or below led to considerable broadening of the resonances and then the appearance of multiple ligand environments. This suggests that several different isomers may exist in solution, perhaps involving C_1 and C_s symmetry (cf. certain bis(phenolate) complexes)[77] and/or additional intra- and/or intermolecular coordination of the tosyl group oxygen atoms as discussed below and noted elsewhere (cf. Figure 2, compound **6**).[60−62,66]

(76) Fletcher, D. A.; McMeeking, R. F.; Parkin, D. *J. Chem. Inf. Comput. Sci.* **1996**, *36*, 746 (The United Kingdom Chemical Database Service).

(77) Toupance, T.; Dubberley, S. R.; Rees, N. H.; Tyrrell, B. R.; Mountford, P. *Organometallics* **2002**, *21*, 1367–1382.

Scheme 1. Synthesis of the New Complexes **10**−**15**

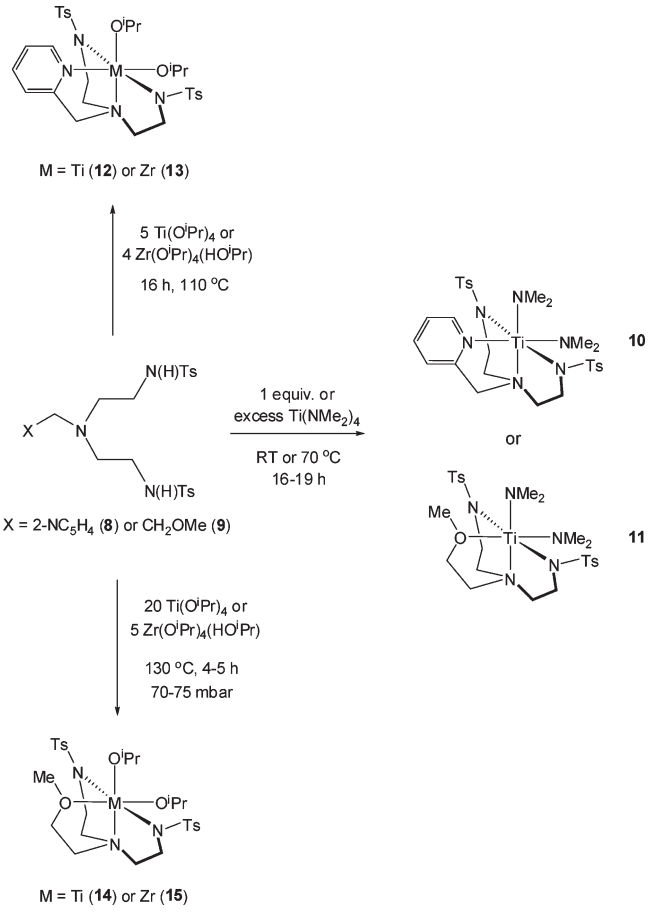

As described below, these bis(dimethylamide) compounds were poor catalysts for the ROP of ε-CL and *rac*-LA, and so we focused our further efforts on their bis(isopropoxide) homologues, $M(L^{py})(O^iPr)_2$ (M = Ti (**12**) or Zr (**13**)) and $M(L^{OMe})(O^iPr)_2$ (M = Ti (**14**) or Zr (**15**)) (Scheme 1). Attempted stoichiometric reaction of H_2L^{py} (**8**) with $Ti(O^iPr)_4$ did not proceed at any appreciable rate at ambient temperature, presumably reflecting the reduced basicity of isopropoxide compared to dimethylamide in the respective titanium starting materials. Nonetheless, heating **8** with an excess of $Ti(O^iPr)_4$ in toluene for 16 h gave good yields of **12** after recrystallization. The zirconium congener **13** was prepared in 42% recrystallized yield in an analogous fashion using an excess of $Zr(^iOPr)_4\cdot HO^iPr$. However, the L^{OMe}-substituted analogues **14** and **15** could not be obtained by the solution reaction of H_2L^{OMe}, even when using large excesses of $Ti(O^iPr)_4$ or $Zr(^iOPr)_4\cdot HO^iPr$ and extended reaction times. This highlights the equilibrium nature of these alcohol-elimination reactions and the apparent need for a strong σ-donor to aid complexation to the metal. Compounds **14** and **15** were eventually prepared using melt conditions at 125−130 °C for 4−5 h under a dynamic partial pressure to remove the eliminated ^iPrOH. Recrystallization afforded the pure complexes in about 45% yield. As for **10**, the NMR spectra of the zirconium complexes showed evidence of complex solution state dynamic behavior. The molecular structures of all four complexes **12**− **15** were therefore determined (vide infra) and again support the structures depicted in Scheme 1.

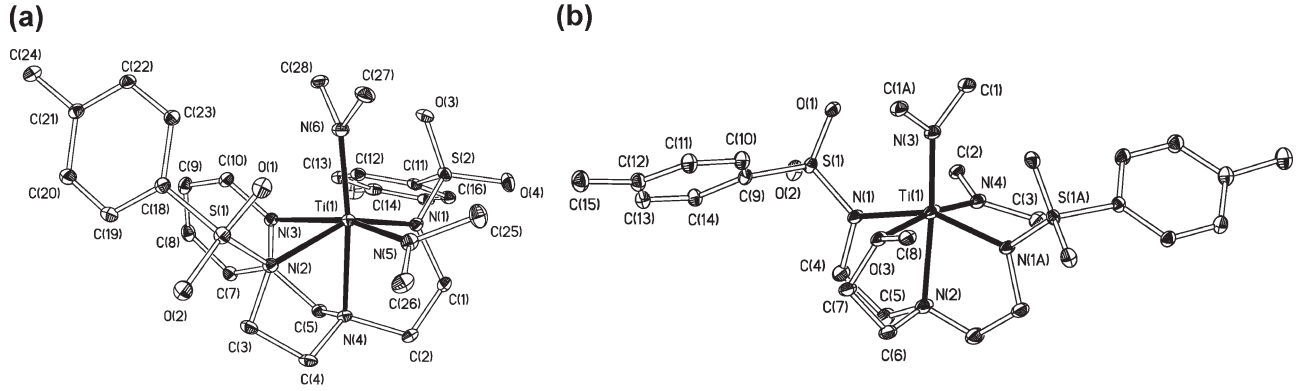

Figure 4. (a) Displacement ellipsoid plot of $Ti(L^{py})(NMe_2)_2$ (**10**). (b) Displacement ellipsoid plot of $Ti(L^{OMe})(NMe_2)_2$ (**11**) where atoms carrying the suffix "A" are related to their counterparts by the symmetry operator $-x, y, -z + 3/2$. Ellipsoids are drawn at the 20% probablility level. H atoms and benzene molecules of crystallization and elements of disorder (for **11**) are omitted for clarity.

As shown in eq 1, $Ti(L^{py})(O^iPr)_2$ (**12**) and $Ti(L^{OMe})(O^iPr)_2$ (**14**) could also be prepared from $Ti(NMe_2)_2(O^iPr)_2$ and 1 equiv of the respective protio-ligand. No evidence for the formation of the bis(dimethylamide) complexes **10** or **11** was found in either case. Compound **14** was isolated in 78% yield on the preparative scale after 2 h reaction time. An NMR tube scale reaction showed quantitative formation of **12** for the corresponding reaction with H_2L^{py} (**8**).

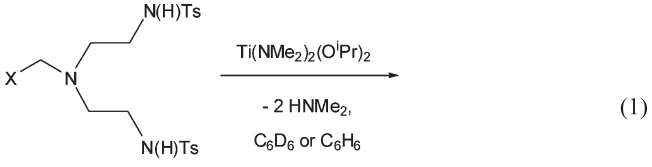

(1)

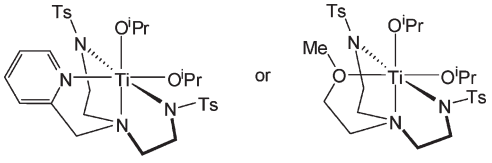

12 **14**

Solid State Structures. The X-ray structures of all six complexes **10**−**15** have been determined. We discuss first the four titanium compounds **10**−**12** and **14**. The molecular structures are shown in Figures 4 and 5, and selected distances and angles are listed in Tables 2 −5. All four possess pseudo-octahedral titanium centers and approximately C_s molecular symmetry, consistent with the fast-exchange limiting NMR spectra discussed above. In general terms the metric parameters lie within the expected ranges to the types of linkages and functional groups present.[76] Unlike many of the previous titanium structures with bi- and tridentate bis(sulfonamide) ligands,[60−62,66,67] none of these structures contain additional Ti···O interaction to the tosyl substituents.

The average $Ti-N_{Ts}$ distance in **10**−**12** and **14** (av. 2.096 Å, range 2.069(5)−2.129(2) Å) is slightly longer than the values reported previously (av. 2.078 Å, range 2.039−2.119 Å). The average $Ti-N_{Ts}$ distance of 2.108 Å in the bis(dimethylamide) complexes **10** and **11** is longer than in the bis(isopropoxide) homologues (av. 2.086 Å) consistent with the better donor ability of NMe_2 compared with that of O^iPr. Consistent with previous structural studies, the average $Ti-NMe_2$ distance of 1.909 Å in **10** and **11** is substantially shorter than the average $Ti-N_{Ts}$ distance, due mainly to the electron-withdrawing nature of the $-SO_2Tol$ substituents. As in other poly(amide) early transition metal structures,[78,79] the various amide ligand substituents in **10** and **11** are arranged so as to maximize $2p_\pi$-$3d_\pi$ bonding interactions. Only one six-coordinate bis(phenolate)-diamine analogue of **10** and **11** has been structurally authenticated, namely, $Ti(O_2{}^{tBu}N^{py})(NMe_2)_2$ (**16**).[80] The overall geometries of **10** and **11** are comparable with that of **16**, with the $Ti-NMe_2$ distances in **10** (1.912(2), 1.916(2) Å) being slightly shorter than in the bis(phenolate) analogue (1.927(3), 1.940(3) Å).

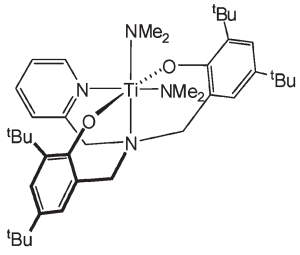

16

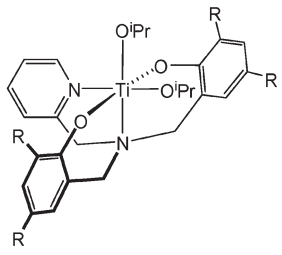

17

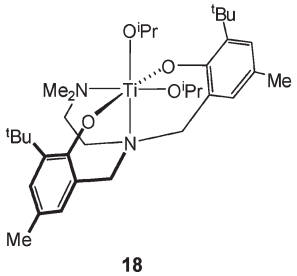

18

Comparisons can be made between $Ti(L^{py})(O^iPr)_2$ (**12**) and $Ti(L^{OMe})(O^iPr)_2$ (**14**) and about 40 structurally characterized, six-coordinate bis(phenolate)-supported

(78) Selby, J. D.; Manley, C. D.; Schwarz, A. D.; Clot, E.; Mountford, P. *Organometallics* **2008**, *27*, 6479–6494.
(79) Ward, B. D.; Orde, G.; Clot, E.; Cowley, A. R.; Gade, L. H.; Mountford, P. *Organometallics* **2004**, *23*, 4444–4461.
(80) Boyd, C. L.; Toupance, T.; Tyrrell, B. R.; Ward, B. D.; Wilson, C. R.; Cowley, A. R.; Mountford, P. *Organometallics* **2005**, *24*, 309–330.

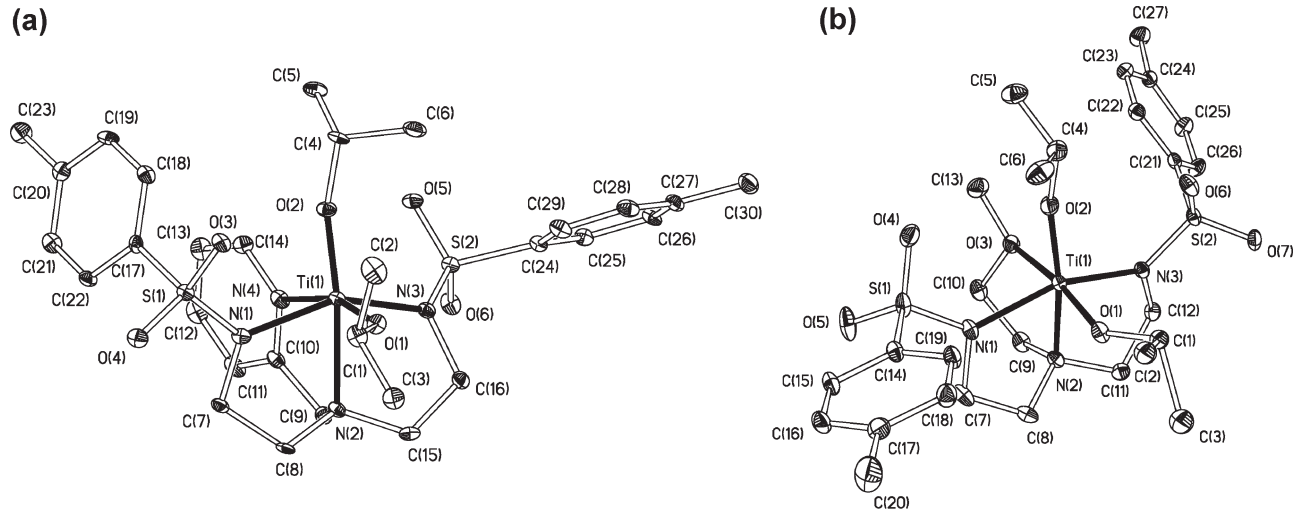

Figure 5. (a) Displacement ellipsoid plot of $Ti(L^{py})(O^iPr)_2$ (**12**). (b) Displacement ellipsoid plot of $Ti(L^{OMe})(O^iPr)_2$ (**14**). Ellipsoids are drawn at the 20% probablility level, and H atoms are omitted for clarity.

Table 2. Selected Bond Distances (Å) and Angles (deg) for $Ti(L^{py})(NMe_2)_2$ (**10**)

Ti(1)−N(1)	2.129(2)	Ti(1)−N(6)	1.916(2)
Ti(1)−N(2)	2.099(2)	S(1)−O(1)	1.439(2)
Ti(1)−N(3)	2.369(2)	S(1)−O(2)	1.447(2)
Ti(1)−N(4)	2.282(2)	S(2)−O(3)	1.439(2)
Ti(1)−N(5)	1.912(2)	S(2)−O(4)	1.445(2)
Ti(1)−N(1)−S(2)	131.72(11)	Ti(1)−N(5)−C(25)	120.4(2)
Ti(1)−N(1)−C(1)	117.2(2)	Ti(1)−N(5)−C(26)	131.0(2)
S(2)−N(1)−C(1)	110.9(2)	C(25)−N(5)−C(26)	108.5(2)
Ti(1)−N(2)−S(1)	127.40(12)	Ti(1)−N(6)−C(27)	122.2(2)
Ti(1)−N(2)−C(3)	116.4(2)	Ti(1)−N(6)−C(28)	129.9(2)
S(1)−N(2)−C(3)	115.7(2)	C(27)−N(6)−C(28)	107.6(2)

Table 3. Selected Bond Distances (Å) and Angles (deg) for $Ti(L^{OMe})(NMe_2)_2$ (**11**)[a]

Ti(1)−N(1)	2.096(4)	Ti(1)−O(3)	2.267(7)
Ti(1)−N(2)	2.201(7)	S(1)−O(1)	1.439(4)
Ti(1)−N(3)	1.898(6)	S(1)−O(2)	1.452(3)
Ti(1)−N(4)	1.981(7)		
Ti(1)−N(1)−S(1)	129.6(2)	Ti(1)−N(4)−C(2)	123.1(9)
Ti(1)−N(1)−C(4)	118.1(3)	Ti(1)−N(4)−C(3)	136.1(9)
S(1)−N(1)−C(4)	112.2(3)	C(2)−N(4)−C(3)	100.0(9)
Ti(1)−N(3)−C(1)	125.8(3)	Ti(1)−O(3)−C(8)	120.1(10)
C(1)−N(3)−C(1A)	108.4(6)		

[a] Atoms carrying the suffix "A" are related to their counterparts by the symmetry operator $-x, y, -z + 3/2$.

Table 4. Selected Bond Distances (Å) and Angles (deg) for $Ti(L^{py})(O^iPr)_2$ (**12**)

Ti(1)−O(1)	1.810(4)	Ti(1)−N(4)	2.278(6)
Ti(1)−O(2)	1.741(4)	S(1)−O(3)	1.429(4)
Ti(1)−N(1)	2.098(5)	S(1)−O(4)	1.447(4)
Ti(1)−N(2)	2.264(5)	S(2)−O(5)	1.433(5)
Ti(1)−N(3)	2.069(5)	S(2)−O(6)	1.444(5)
Ti(1)−O(1)−C(1)	139.2(4)	S(1)−N(1)−C(7)	117.3(4)
Ti(1)−O(2)−C(4)	159.7(4)	Ti(1)−N(3)−S(2)	127.1(3)
Ti(1)−N(1)−S(1)	125.0(3)	Ti(1)−N(3)−C(16)	116.3(4)
Ti(1)−N(1)−C(7)	117.4(4)	S(2)−N(3)−C(16)	113.4(4)

bis(isopropoxide) complexes in general,[76] including $Ti(O_2{}^RN^{py})(O^iPr)_2$ (**17**, R = Me or ^{t}Bu) and $Ti(O_2{}^RN^{Me_2})(O^iPr)_2$ (**18**) specifically.[41,42] The overall geometries are comparable, as are the Ti−O−^{i}Pr angles (literature range 127−168°, av. 143°; for **12** and **14** range 139.2(4)−159.7(4)°, av. 150°). However, the Ti−O^{i}Pr distances are, as for the Ti−NMe_2 distances discussed above, shorter in the

Table 5. Selected Bond Distances (Å) and Angles (deg) for $Ti(L^{OMe})(O^iPr)_2$ (**14**)

Ti(1)−O(1)	1.7920(18)	Ti(1)−N(3)	2.0873(19)
Ti(1)−O(2)	1.7534(18)	S(1)−O(4)	1.436(2)
Ti(1)−O(3)	2.3271(18)	S(1)−O(5)	1.445(2)
Ti(1)−N(1)	2.091(2)	S(2)−O(6)	1.4337(18)
Ti(1)−N(2)	2.277(2)	S(2)−O(7)	1.4459(18)
Ti(1)−O(1)−C(1)	146.1(3)	S(1)−N(1)−C(7)	112.28(16)
Ti(1)−O(2)−C(4)	158.09(19)	Ti(1)−N(3)−S(2)	127.23(11)
Ti(1)−O(3)−C(13)	120.41(16)	Ti(1)−N(3)−C(12)	118.28(14)
Ti(1)−N(1)−S(1)	129.25(12)	S(2)−N(3)−C(12)	114.45(15)
Ti(1)−N(1)−C(7)	118.42(16)		

sulfonamide analogues with average values of 1.774 Å compared with a literature value of 1.804 Å (range 1.749−1.852 Å) in general and 1.813 Å (range 1.806−1.832 Å) for **17** and **18**.

The molecular structures of $Zr(L^{py})(O^iPr)_2$ (**13**) and $Zr(L^{OMe})(O^iPr)_2$ (**15**) are shown in Figure 6, and selected bond distances and angles are listed in Tables 6 and 7. Crystals of **15** are isomorphous with those of **14**, and the molecular geometries are essentially identical. Five six-coordinate bis(phenolate)-supported analogues of **15** have been structurally characterized, including the zirconium congeners of **17** and **18**.[41,42] Their geometries are again all comparable to that of **15** but the Zr−O^{i}Pr bond lengths in the latter (1.910(2), 1.911(2) Å) are shorter than the bis(phenolate) examples (av. 1.943 Å, range 1.910−1.967 Å). This parallels the trends found in the titanium systems.

Only one monomeric zirconium sulfonamide compound has been structurally characterized previously, namely, the seven-coordinate $Zr\{1,2\text{-}C_6H_{10}(NTs)_2\}(NMe_2)_2(NHMe_2)$ (Figure 2) which possesses two $\kappa^2(N,O)$ bound NTs groups. As mentioned, this $\kappa^2(N,O)$ coordination mode of NSO_2R groups is very common for Group 4 and other electron-deficient metals. As can be seen from Figure 6, $Zr(L^{py})(O^iPr)_2$ (**13**) possesses one $\kappa^2(N,O)$ bound NTs group giving an unsymmetrical seven-coordinate metal center. This is in contrast to the C_s, six-coordinate geometry of its congener, **12** (presumably because of the smaller atomic radius of titanium), and also **15**. However, the complicated solution phase NMR spectra mentioned above for **12**, **14**, and

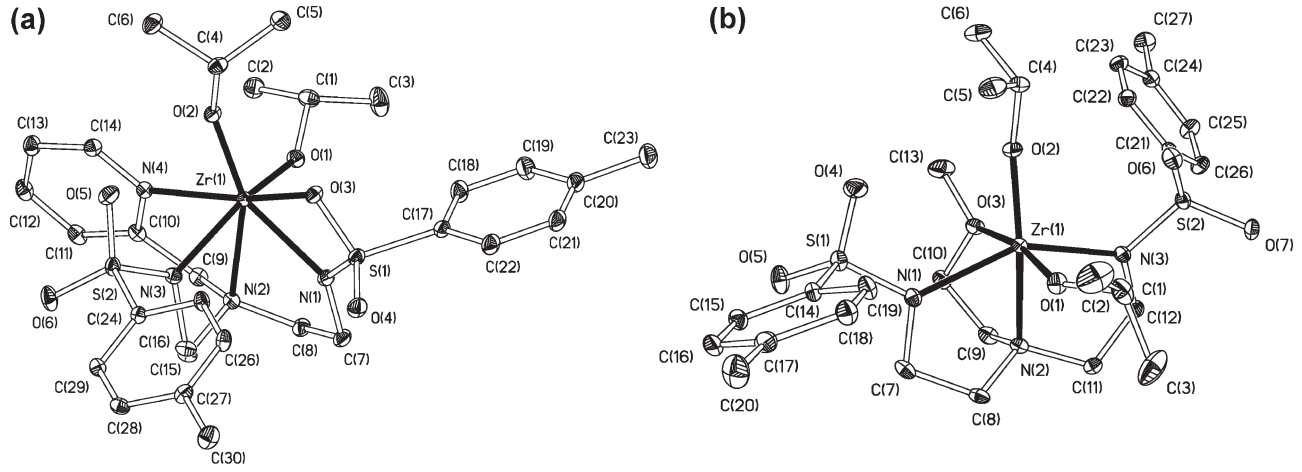

Figure 6. (a) Displacement ellipsoid plot of $Zr(L^{py})(O^iPr)_2$ (**13**). (b) Displacement ellipsoid plot of $Zr(L^{OMe})(O^iPr)_2$ (**15**). Ellipsoids are drawn at the 20% probablility level, and H atoms are omitted for clarity.

Table 6. Selected Bond Distances (Å) and Angles (deg) for $Zr(L^{py})(O^iPr)_2$ (**13**)

Zr(1)−O(1)	1.9644(16)	Zr(1)−N(4)	2.3880(19)
Zr(1)−O(2)	1.9260(16)	S(1)−O(3)	1.4881(17)
Zr(1)−O(3)	2.3498(16)	S(1)−O(4)	1.4370(18)
Zr(1)−N(1)	2.2332(19)	S(2)−O(5)	1.435(2)
Zr(1)−N(2)	2.4933(19)	S(2)−O(6)	1.4536(19)
Zr(1)−N(3)	2.2779(19)		
Zr(1)−O(1)−C(1)	145.76(16)	S(1)−N(1)−C(7)	128.20(17)
Zr(1)−O(2)−C(4)	148.07(15)	Zr(1)−N(3)−S(2)	132.48(11)
Zr(1)−O(3)−S(1)	99.27(8)	Zr(1)−N(3)−C(16)	113.47(14)
Zr(1)−N(1)−S(1)	102.18(10)	S(2)−N(3)−C(16)	114.03(16)
Zr(1)−N(1)−C(7)	129.31(15)		

Table 7. Selected Bond Distances (Å) and Angles (deg) for $Zr(L^{OMe})(O^iPr)_2$ (**15**)

Zr(1)−O(1)	1.910(2)	Zr(1)−N(3)	2.216(2)
Zr(1)−O(2)	1.911(2)	S(1)−O(4)	1.440(3)
Zr(1)−O(3)	2.393(2)	S(1)−O(5)	1.441(2)
Zr(1)−N(1)	2.227(3)	S(2)−O(6)	1.439(2)
Zr(1)−N(2)	2.434(3)	S(2)−O(7)	1.444(2)
Zr(1)−O(1)−C(1)	148.4(3)	S(1)−N(1)−C(7)	115.1(2)
Zr(1)−O(2)−C(4)	155.3(2)	Zr(1)−N(3)−S(2)	122.23(14)
Zr(1)−O(3)−C(13)	120.3(2)	Zr(1)−N(3)−C(12)	121.06(19)
Zr(1)−N(1)−S(1)	123.56(15)	S(2)−N(3)−C(12)	116.7(2)
Zr(1)−N(1)−C(7)	121.33(19)		

15 imply that several more coordination geometries may be accessible in solution. The Zr−O^{i}Pr and Zr−N distances in **13** are all longer than the corresponding ones in **15** reflecting the higher coordination number of the former. The S(1)−O(3) distance for the bridging sulfonamide oxygen is 0.051(3) Å longer than the terminal S(1)−O(4) bond as expected.

Overall the geometries of **10**−**15** parallel those of the well-established bis(phenolate) complexes but with slightly shorter Ti−NMe_2 and M−O^{i}Pr distances and the potential in both the solid state and solution for additional stabilization of the metal centers via M···O_{Ts} interactions.

Polymerization Studies: ROP of ε-CL. A principal aim of this work was to evaluate the potential of sulfonamide-supported Group 4 complexes for the catalytic ROP of ε-CL and *rac*-LA. An initial study using the six compounds **10**−**15** was undertaken using ε-CL because of the relative ease of its polymerization due to the favorable release of 7-membered ring strain. Initial studies performed in tetrahydrofuran (THF) gave extremely long reaction times and negligible conversions, presumably because of THF competition for coordination to the metal center. Subsequent studies were performed in toluene at 100 °C, and under these conditions all the complexes were found to be active. The progress of each reaction was monitored by regular sampling, and the results summarized in Table 8 correspond to when the polymerizations eventually reached 100% conversion. The molecular weights and PDIs (M_w/M_n) were determined by gel permeation chromotography (GPC) using the appropriate Mark−Houwink corrections,[81−83] and the yield refers to the amount of poly(ε-CL) isolated. The M_n(calcd) values are those expected for two polymer chains growing per metal center (i.e., one chain per Ti−NMe_2 or M−O^{i}Pr bond in the starting complex) at 100% conversion of monomer.

Table 8. Solution Polymerization of ε-CL by $Ti(L^{py})(NMe_2)_2$ (**10**), $Ti(L^{OMe})(NMe_2)_2$ (**11**), $Ti(L^{py})(O^iPr)_2$ (**12**), $Zr(L^{py})(O^iPr)_2$ (**13**), $Ti(L^{OMe})(O^iPr)_2$ (**14**), and $Zr(L^{OMe})(O^iPr)_2$ (**15**)[a]

catalyst	yield (%)[b]	time (h)	M_n (GPC)[c]	M_n (calcd)[d]	M_w/M_n
$Ti(L^{py})(NMe_2)_2$ (**10**)	97	12	12,990	5,710	1.91
$Ti(L^{OMe})(NMe_2)_2$ (**11**)	95	22	14,260	5,710	1.60
$Ti(L^{py})(O^iPr)_2$ (**12**)	93	9	5,720	5,710	1.80
$Ti(L^{OMe})(O^iPr)_2$ (**14**)	87	1	6,390	5,710	1.39
$Zr(L^{py})(O^iPr)_2$ (**13**)	91	1	5,180	5,710	1.19
$Zr(L^{OMe})(O^iPr)_2$ (**15**)	93	1	7,770	5,710	1.18

[a] Conditions: [ε-CL]/[catalyst] = 100:1, 6.8 mL of toluene at 100 °C. See Experimental Section for other details. [b] Isolated yield at 100% NMR conversion. [c] Molecular weights (g mol^{-1}) determined from GPC using the appropriate Mark−Houwink corrections. [d] Expected M_n (g mol^{-1}) for 2 chains growing per metal center at 100% conversion. For one chain per metal center the calculated value is 11,410 g mol^{-1}.

The bis(dimethylamide) catalysts $Ti(L^R)(NMe_2)_2$ (**10** and **11**) were the slowest of the six evaluated. The GPC data are consistent with only one poly(ε-CL) chain forming per metal (M_n(calcd) = 11,420 g mol^{-1}) on average. This is consistent with the rate of initiation by the expected coordination−insertion mechanism[32] (insertion of ε-CL

(81) Alfred, R.; Howard, L. W. H. *J. Polym. Sci., Part A: Polym. Chem.* **1972**, *10*, 217–235.
(82) Barakat, I.; Ph D.; Jérôme, R.; Ph T. *J. Polym. Sci., Part A: Polym. Chem.* **1993**, *31*, 505–514.
(83) John, R. D.; Jay, J.; Daniel, M. K.; Sukhendu, B. H.; Bradford, R. L.; Matthew, H. H. *J. Polym. Sci., Part B: Polym. Phys.* **2005**, *43*, 3100–3111.

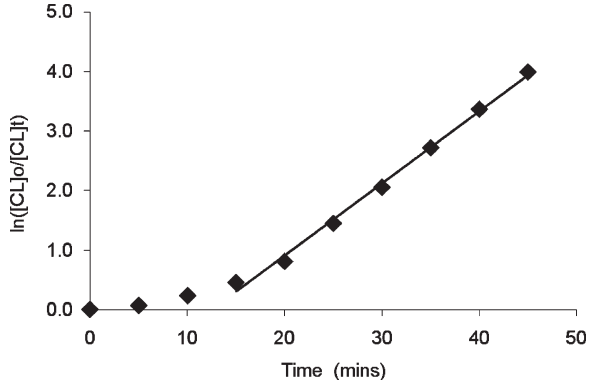

Figure 7. First order plot for ε-CL consumption using $Zr(L^{OMe})(O^iPr)_2$ (**15**). Conditions: [ε-CL_0]/[**15**] = 100:1, 6.8 mL of toluene, 100 °C, 0.1 mL aliquots taken at the given intervals. See Experimental Section for other details. Linear fit (r^2 = 0.995) shown is for the first order region after the induction period. See the Supporting Information for corresponding plots for **12**, **13**, and **14**.

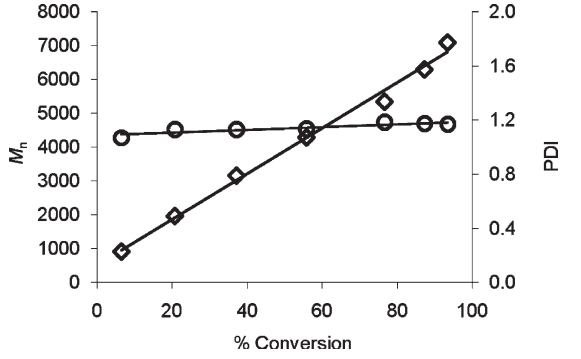

Figure 8. Plots of M_n and PDI (determined by GPC) vs conversion for the polymerization of ε-CL using $Zr(L^{OMe})(O^iPr)_2$ (**15**). Conditions: [ε-CL_0]/[**15**] = 100:1, 6.8 mL of toluene, 100 °C, 0.1 mL aliquots taken at the given intervals. Hollow diamonds correspond to M_n and hollow circles to PDI.

into Ti−NMe_2) being much slower than propagation (insertion of subsequent ε-CLs into the growing Ti−$\{O(CH_2)_5C(O)\}_nNMe_2$ chain). Analogous effects have been recorded elsewhere.[50] Although the observed and calculated M_n values for the poly(ε-CL) formed with **10** and **11** are in fairly good agreement for a living-type process, the broad PDIs of 1.91 and 1.60 show that there is poor control in terms of the distribution of molecular weights. Our further efforts therefore focused on the bis(isopropoxide) systems.

Changing from $Ti(L^R)(NMe_2)_2$ (**10** and **11**) to $Ti(L^R)(O^iPr)_2$ (**12** and **14**) gave a clear switch from about one to two poly(ε-CL) chains per metal center and also (especially for **14**) a significant increase in activity. The zirconium analogues **13** and **15** were, according to the primary screen in Table 8, at least as productive as **14**, also forming two chains per metal center. In addition, the PDI values for these two catalysts indicated a better controlled polymerization process than for any of the titanium systems. ^{1}H NMR and MALDI-ToF-MS analysis (see the Supporting Information for examples) of all four poly(ε-CL)s showed one O^iPr end group per chain, consistent with a coordination−insertion mechanism.[32] Further experiments were carried out with **12**−**15** to evaluate the kinetic behavior and first order rates of propagation, and also how M_n increases with conversion.

Table 9. First Order Propagation Rate Constant (k_p) for ε-CL Polymerization by $Ti(L^{py})(O^iPr)_2$ (**12**), $Zr(L^{py})(O^iPr)_2$ (**13**), $Ti(L^{OMe})(O^iPr)_2$ (**14**), and $Zr(L^{OMe})(O^iPr)_2$ (**15**)[a]

catalyst	k_p (min^{-1})
$Ti(L^{py})(O^iPr)_2$ (**12**)	0.0075(7)
$Ti(L^{OMe})(O^iPr)_2$ (**14**)	0.065(3)
$Zr(L^{py})(O^iPr)_2$ (**13**)	0.108(5)
$Zr(L^{OMe})(O^iPr)_2$ (**15**)	0.121(4)

[a] Conditions: [ε-CL_0]/[$M(L^R)(O^iPr)_2$] = 100:1, 6.8 mL of toluene, 100 °C.

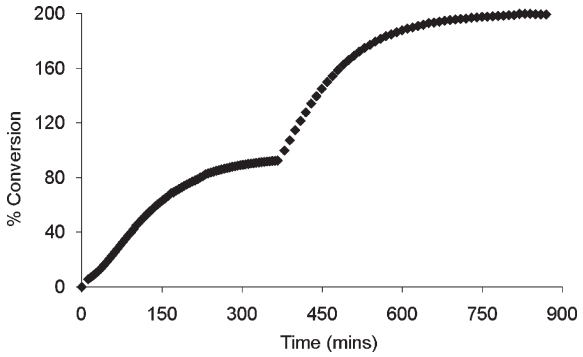

Figure 9. Plot of % conversion vs time for the polymerization of two consecutive batches of ε-CL using $Zr(L^{OMe})(O^iPr)_2$ (**15**). Conditions [CL_0]/[**15**] = 100:1 followed by a further 100 equiv at t = 400 min, 0.75 mL of C_6D_6, 70 °C.

Representative plots are shown in Figures 7 and 8 for $Zr(L^{OMe})(O^iPr)_2$ (**15**). Analogous plots for **12**−**14** are shown in the Supporting Information. First order propagation rate constants (k_p) obtained from the linear part of the log plots are given in Table 9.

Catalysts **13**−**15** show a relatively short induction period of 5−10 min followed by a polymerization process that is first order with respect to ε-CL concentration (Figure 7). Similar induction periods have been observed for main group and transition metal isopropoxide catalysts.[20,42,84] The induction period for $Ti(L^{py})(O^iPr)_2$ (**12**, see the Supporting Information) was substantially longer (ca. 60−70 min) than the other three. The k_p values (Table 9) show two main features. First, as found for the corresponding bis(phenolate) systems,[41,42] the zirconium catalysts are faster than the titanium ones for a given L^R supporting ligand. Second, there is a pendant arm effect for both pairs of catalyst with the k_p values for L^{py}-supported systems being less than for their L^{OMe} analogues (considerably so in the case of **12** and **14**). We interpret both of these effects in terms of easier access to the metal center since Zr is larger than Ti and OMe is a more labile donor than pyridyl.

Catalysts **13**, **14**, and **15** gave reasonably linear plots of M_n versus % conversion (Figure 8 and the Supporting Information) with narrow PDIs (1.10−1.20 for **13** and **15**, somewhat broader for the less well-behaved **14**) which remained effectively constant throughout the process. The gradients of the M_n versus % conversion plots were 47(2), 64(4), and 67(3) g mol^{-1} (% conversion)$^{-1}$ (av. 59 g mol^{-1} (% conversion)$^{-1}$) which are close to that expected (57 g mol^{-1} (% conversion)$^{-1}$) for two poly(ε-CL) chains growing per metal center. All of these data are consistent

(84) Duda, A.; Penczek, S. *Macromolecules* **1995**, *28*, 5981–5992.

with these species acting as living catalysts for ROP of ε-CL.

To make a proper comparison with previously reported bis(phenolate)amine systems, we also evaluated Davidson et al.'s[57] ROP catalyst $Zr(O_2{}^{Me}N^{py})(O^iPr)_2$ (**19**) under the same conditions as **12**−**15**. This had a slightly shorter induction period (5 min) and a k_p of 0.226(8) s^{-1}. The k_p for compound **19** is therefore twice that of the most comparable bis(sulfonamide) catalyst **13** (k_p = 0.108(5) s^{-1}). However, the corresponding sulfonamide demonstrated a more controlled polymerization process with a M_n of 5,180 g mol^{-1} and a PDI of 1.19 compared to **19** which yielded poly(ε-CL) with a M_n of 8,000 g mol^{-1} and a PDI of 1.55, where the calculated value of M_n for 2 chains per metal center is 5,710 g mol^{-1}.

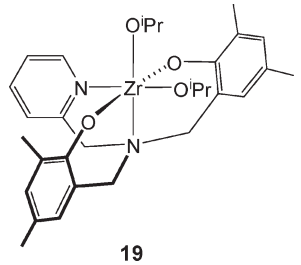

19

As a final probe of the living characteristics of the most active catalyst, namely, **15**, polymerization resumption experiments were undertaken in which 100 equiv of ε-CL were polymerized on the NMR tube scale at 70 °C in C_6D_6. Once full conversion had been observed, a further 100 equiv were added, and the reaction once again was monitored until completion (Figure 9). Consistent with Figure 7, the data in Figure 9 indicate a short induction period before becoming first order in monomer concentration (see the Supporting Information for the corresponding semilogarithmic plots). Interestingly, the second 100 equiv of monomer show minimal induction period, presumably because the active catalyst is fully formed after the initial polymerization and is still "living". The k_p values for both parts of Figure 9 (i.e., the first and second portions of ε-CL) are identical at 0.009(1) min^{-1}. GPC analysis of the poly(ε-CL) showed a narrow PDI (1.19) and an M_n of 9,980 g mol^{-1} which is in reasonable agreement with the M_n(calcd) value of 11,410 g mol^{-1} for two chains per metal center.

Polymerization Studies: ROP of *rac*-LA. The studies of the ROP of ε-CL showed $Zr(L^{py})(O^iPr)_2$ (**13**) and $Zr(L^{OMe})(O^iPr)_2$ (**15**) to be the best catalysts in terms of activity and polymerization control. Our studies were next extended to the more challenging monomer, *rac*-LA. Preliminary experiments showed **15** to be significantly more active than **13**, but with otherwise similar ROP features (control of M_n, PDI). We therefore focused on **15** for detailed studies. Solution polymerizations were performed in toluene at 70 °C until about 95% completion. As shown in Figure 10 the polymerization follows first order consumption of *rac*-LA (k_p = 0.0076(2) min^{-1}) and there is again a noticeable induction period.[20,42,84]

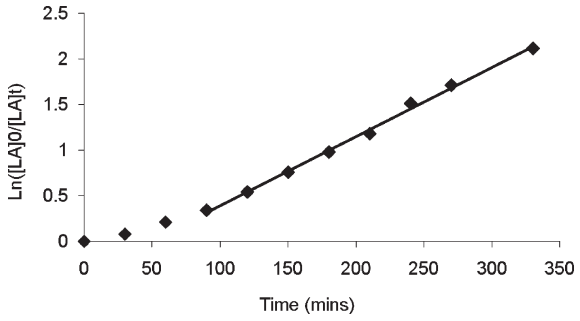

Figure 10. First order plot for *rac*-LA consumption using $Zr(L^{OMe})(O^iPr)_2$ (**15**). Conditions [*rac*-LA_0]/[**15**] = 100:1, 6 mL of toluene, 70 °C, 0.1 mL aliquots taken at the given intervals. See Experimental Section for other details. Linear fit (r^2 = 0.996) shown is for the first order region after the induction period.

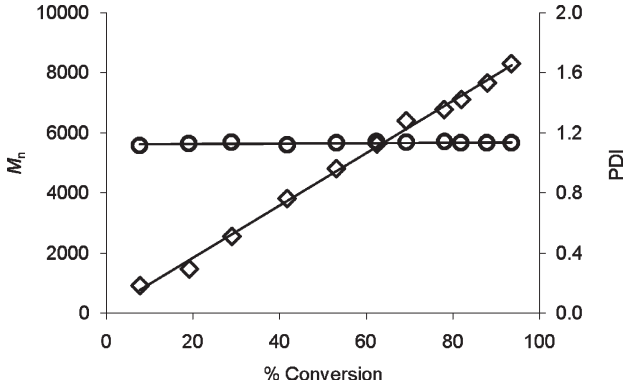

Figure 11. Plots of M_n and PDI (determined by GPC) vs conversion for the solution polymerization of *rac*-LA using $Zr(L^{OMe})(O^iPr)_2$ (**15**). Conditions: [*rac*-LA_0]/[**15**] = 100:1, 6.0 mL of toluene, 70 °C, 0.1 mL aliquots taken at the given intervals. Hollow diamonds correspond to M_n and hollow circles to PDI.

Figure 11 shows that M_n increases linearly with conversion in a living fashion. The final experimental M_n (94% conversion) of 8,290 g mol^{-1} is in good agreement with the expected value of 6,740 g mol^{-1} if two *rac*-LA chains were growing per metal center. The gradient of the plot is 88(1) g mol^{-1} (% conversion)$^{-1}$ which compares favorably with the expected value (72 g mol^{-1} (% conversion)$^{-1}$). Figure 11 also shows that the PDIs remain very narrow and effectively constant between 1.12 and 1.14 throughout the process, consistent with a single site catalyst. The ^{1}H NMR and MALDI-ToF-MS spectra of the poly(*rac*-LA) show the expected single O^iPr end group per chain, consistent with a coordination−insertion mechanism. Unfortunately, the selectively homonuclear decoupled ^{1}H NMR spectrum showed that the polymer was effectively atactic (in accord with the behavior of the corresponding bis(phenolate)amine-supported catalysts) and so under these conditions the bis(sulfonamide) supporting ligand is not able to significantly influence the enchainment preferences of L-LA and D-LA (chain end control). The separation between the *m*/*z* envelopes in the MALDI-TOF-MS (see the Supporting Information) was 72 g mol^{-1} which is half the molecular weight of a single lactidyl unit and therefore indicative of extensive intermolecular transesterification during the polymerization process as is very often observed with metal-based catalysts.

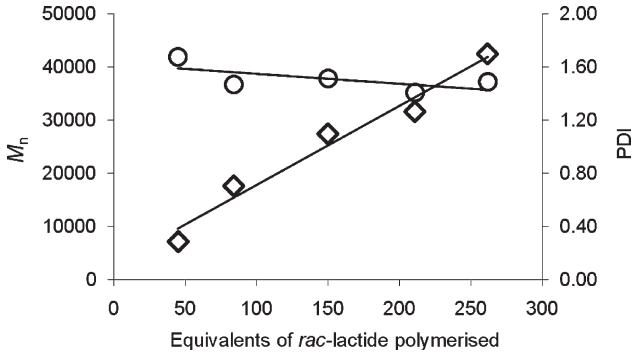

Figure 12. Plots of M_n and PDI (determined by GPC) vs conversion for the melt polymerization of various equivalents of *rac*-LA using $Zr(L^{OMe})(O^iPr)_2$ (**15**). Conditions: [*rac*-LA_0]/[**15**] = various values between 50:1 and 300:1, 130 °C, 30 min. See Experimental Section for other details. Hollow diamonds correspond to M_n and hollow circles to PDI.

Polymerization experiments were also undertaken under industrially relevant melt conditions to evaluate catalyst **15** (Figure 12).[85,86] Excellent conversions (ca. 90%) of between 50 and 300 starting equivalents of *rac*-LA in 30 min at 130 °C were obtained giving atactic, isopropoxy-terminated polymers with M_n values up to 42,430 g mol^{-1} (PDI = 1.49) for the experiment starting with 300 equiv of *rac*-LA. This value compares fairly well with an expected M_n of 37,690 g mol^{-1} for *one* chain per metal. The gradient of the M_n versus equivalents of *rac*-LA polymerized plot (Figure 12) is 149(16) g mol^{-1} $equiv^{-1}$ which is the same within error as the expected value of 144 for one chain per metal center and consistent with a living catalyst. It is not clear why only one chain grows per metal center in the melt compared to two per metal in solution. The polymers had broader PDIs than in the solution experiments (carried out at lower temperature) as expected. Again the poly(*rac*-LA) was predominantly atactic. Nonetheless, the activity of **15** under these conditions is superior to those of the aforementioned bis(phenolate) systems which gave up to 75% conversion over somewhat longer reaction times (2 h),[57] and is comparable to the tris(phenolate) systems of the type **4** in Figure 1 (50 or 95% conversion after 0.5 h (M = Ti or Hf); 78% conversion after 0.1 h (M = Zr) for [*rac*-LA]:[**4**] = 300).[42,54]

Conclusions

In this contribution we have reported the first transition metal sulfonamide-supported catalysts for the ROP of ε-CL and *rac*-LA. The productivities of these new complexes are comparable to those of the well-established and thoroughly explored bis(phenoxide) and related Group 4 analogues. The new bis(amide) complexes $Ti(L^{py})(NMe_2)_2$ (**10**) or $Ti(L^{OMe})(NMe_2)_2$ (**11**) were easily prepared under mild conditions because of the high basicity of the NMe_2 ligand, whereas the bis(isopropoxide) analogues $M(L^{py})(O^iPr)_2$ and $M(L^{OMe})(O^iPr)_2$ (**12**−**15**) required more forcing conditions when starting from the homoleptic precursors. Indeed, it is somewhat surprising that the sulfonamides H_2L^R (**8**, **9**) were able to displace ^{i}PrOH at all, and the reaction conditions required for their synthesis certainly testify to the equilibrium nature of the reactions. The amide complexes **10** and **11** were found to be poor catalysts for the ROP of ε-CL, and long reaction times and poor control were observed. This is attributed to the greater dissimilarity between the initiating group Ti−NMe_2 and the subsequent growing chain Ti−$\{O(CH_2)_5C(O)\}_nNMe_2$, as well as to the smaller radius of Ti compared with Zr. With respect to the Group 4 isopropoxide complexes, the ROP results for ε-CL were in agreement with literature precedent in that the zirconium homologues were more active than their titanium counterparts. Polymerization rates were higher for the catalysts bearing an OMe donor (**14** and **15**) compared to a pyridyl one. The zirconium catalyst **15** was found to be an active and well-controlled catalyst for the living ROP of *rac*-LA both in solution and in the melt. All poly(*rac*-LA)s formed were predominantly atactic. Further work in our laboratory is underway to assess different sulfonamide substituents and ligand backbone motifs to increase catalyst activity and control.

Experimental Section

General Methods and Instrumentation. All manipulations were carried out using standard Schlenk line or drybox techniques under an atmosphere of argon or dinitrogen. Solvents were degassed by sparging with dinitrogen and dried by passing through a column of the appropriate drying agent. Toluene was refluxed over sodium and distilled. Deuterated solvents were dried over sodium (C_6H_6) or P_2O_5 ($CDCl_3$ and CD_2Cl_2), distilled under reduced pressure, and stored under dinitrogen in Teflon valve ampules. NMR samples were prepared under dinitrogen in 5 mm Wilmad 507-PP tubes fitted with J. Young Teflon valves. ^{1}H and ^{13}C-{^{1}H} NMR spectra were recorded on Varian Mercury-VX 300 and Varian Unity Plus 500 spectrometers at ambient temperature unless stated otherwise and referenced internally to residual protio-solvent (^{1}H) or solvent (^{13}C) resonances, and are reported relative to tetramethylsilane (δ = 0 ppm). Assignments were confirmed using two-dimensional ^{1}H−^{1}H and ^{13}C−^{1}H NMR correlation experiments. Chemical shifts are quoted in δ (ppm) and coupling constants in hertz. IR spectra were recorded on a Nicolet Magna 560 ESP FTIR spectrometer. Samples were prepared in a drybox as Nujol mulls between NaCl plates, and the data are quoted in wavenumbers (cm^{-1}). Elemental analyses were carried out by the Elemental Analysis Service at the London Metropolitan University.

MALDI-ToF-MS analysis was performed on a Waters MALDI micro equipped with a 337 nm nitrogen laser. An accelerating voltage of 25 kV was applied. The polymer samples were dissolved in THF at a concentration of 1 mg mL^{-1}. The cationization agent used was potassium trifluoroacetate (Fluka, > 99%) dissolved in THF at a concentration of 5 mg mL^{-1}. The matrix used was *trans*-2-[3-(4-*tert*-butylphenyl)-2-methyl-2-propenylidene]malononitrile (DCTB) (Fluka) and was dissolved in THF at a concentration of 40 mg mL^{-1}. Solutions of matrix, salt, and polymer were mixed in a volume ratio of 4:1:4, respectively. The mixed solution was hand-spotted on a stainless steel MALDI target and left to dry. The spectra were recorded in the refectron mode.

Polymer molecular weights (M_n, M_w) were determined by GPC using a Polymer Laboratories Plgel Mixed-D column (300 mm length, 7.5 mm diameter) and a Polymer Laboratories PL-GPC50 Plus instrument equipped with a refractive index detector. THF (HPLC grade) was used as an eluent at 30 °C with a rate of 1 mL min^{-1}. Linear polystyrenes were used as primary calibration standards, and Mark−Houwink corrections for poly(ε-CL) or poly(*rac*-LA) in THF were applied for the experimental samples.[81−83]

(85) Vink, E. T. H.; Rábago, K. R.; Glassner, D. A.; Gruber, P. R. *Polym. Degrad. Stab.* **2003**, *80*, 403–419.
(86) Drumright, R. E.; Gruber, P. R.; Henton, D. E. *Adv. Mater.* **2000**, *12*, 1841–1846.

Starting Materials. $Ti(NMe_2)_4$,[87,88] $Ti(NMe_2)_2(O^iPr)_2$,[89,90] H_2L^{py} (**8**),[74] and H_2L^{OMe} (**9**)[75] were synthesized according to published procedures. ε-CL was dried over freshly ground CaH_2 and distilled before use. *rac*-LA was recrystallized twice from toluene and then sublimed twice prior to use. Other reagents were purchased from Sigma-Aldrich and used without further purification.

$Ti(L^{py})(NMe_2)_2$ (10). A slurry of H_2L^{py} (0.25 g, 0.50 mmol) in benzene (30 mL) was added to a solution of $Ti(NMe_2)_4$ (0.12 mL, 0.50 mmol) in benzene (10 mL). The mixture was stirred for 19 h, resulting in a dark red solution with brown percipitate. The solid was filtered off and washed with pentane (3 × 30 mL). Recrystallization from a saturated benzene solution yielded **10** as a brick-red solid that was washed with pentane (3 × 20 mL) and dried in vacuo. Yield: 0.17 g (55%). ^{1}H NMR (CD_2Cl_2, 299.9 MHz, 303 K): δ 8.91 (1H, m, 2-NC_5H_4), 8.31 (1H, m, 4-NC_5H_4), 7.78 (1H, app. t, ^3J = 6.9 Hz, 3-NC_5H_4), 7.52 (1H, d, ^3J = 4.3 Hz, 2-C_6H_4Me), 7.20 (1H, m, 5-NC_5H_4), 7.12 (1H, d, ^3J = 4.5 Hz, 3-C_6H_4Me), 3.79 (6H, s, NMe_2 *cis* to py), 3.59 (4H, br. m, overlapping $pyCH_2$ and $TsNCH_2$), 3.44 (6H, br. s, NMe_2 *trans* to py), 3.21 (2H, br. m, $TsNCH_2CH_2$), 2.87 (4H, br. m, $TsNCH_2CH_2$), 2.37 (6H, s, C_6H_4Me) ppm. A satisfactory ^{13}C NMR spectrum could not be obtained because of the fluxional nature of the compound. IR: 3464 (w), 1255 (w), 1143 (m), 1088 (m), 947 (m), 665 (m), 511 (w) cm^{-1}. Anal. found (calcd. for $C_{28}H_{40}N_6O_4S_2Ti$): C, 52.85 (52.82); H, 6.33 (6.26); N, 13.15 (13.20) %.

$Ti(L^{OMe})(NMe_2)_2$ (11). A slurry of H_2L^{OMe} (0.16 g, 0.34 mmol) in benzene (60 mL) was added to a solution of $Ti(NMe_2)_4$ (0.6 mL, 2.54 mmol) in benzene (20 mL). The mixture was heated at 70 °C for 16 h, resulting in a dark red solution. Removal of the volatiles under reduced pressure yielded a dark red solid that was recrystallized from a concentrated benzene solution to yield **11** as a red solid which was washed with pentane (3 × 20 mL) and dried in vacuo. Yield: 0.11 g (51%). ^{1}H NMR (CD_2Cl_2, 299.9 MHz): δ 7.72 (4H, d, ^3J = 6.1 Hz, 2-C_6H_4Me), 7.29 (4H, d, ^3J = 6.1 Hz, 3-C_6H_4Me), 3.54 (6H, s, NMe_2 *cis* to OMe), 3.43−3.34 (9H, m, overlapping OMe, OCH_2 and $TsNCH_2$), 3.20 (6H, s, NMe_2 *trans* to OMe), 2.82 (6H, m, overlapping OCH_2CH_2 and $TsNCH_2CH_2$), 2.40 (6H, s, C_6H_4Me). ^{13}C-{^{1}H} NMR (CD_2Cl_2, 75.4 MHz): δ 141.8 (1-C_6H_4Me), 140.4 (4-C_6H_4Me), 130.4 (3-C_6H_4Me), 127.9 (2-C_6H_4Me), 69.7 ($TsNCH_2$), 61.3 (OCH_2), 55.7 ($TsNCH_2CH_2$), 51.4 (OCH_2CH_2), 49.6 (*cis* to OMe NMe_2), 49.5 ($TsNCH_2$), 49.3 (NMe_2 *trans* to OMe), 21.6 (C_6H_4Me). IR: 3446 (w) 1302 (m), 1295 (w), 1284 (m), 1139 (m), 1020 (s), 943 (s), 864 (m), 666 (m), 554 (w) cm^{-1}. Anal. found (calcd. for $C_{25}H_{41}N_5O_5S_2Ti$); C, 49.60 (49.74); H, 6.94 (6.85); N, 11.48 (11.60) %.

$Ti(L^{py})(O^iPr)_2$ (12). A slurry of H_2L^{py} (0.75 g, 1.50 mmol) in toluene (50 mL) was added to a solution of $Ti(O^iPr)_4$ (2.2 mL, 7.5 mmol) in toluene (20 mL). The mixture was heated at 100 °C for 16 h, resulting in an off-white slurry. The solid was filtered off and washed with pentane (3 × 30 mL). Recrystallization from a saturated dichloromethane solution layered with pentane yielded **12** as a beige solid that was washed with hexanes (3 × 20 mL) and dried in vacuo. Yield: 0.62 g (62%). ^{1}H NMR (CD_2Cl_2, 299.9 MHz): δ 8.76 (1H, dd, ^3J = 4.7 Hz, ^4J = 6.0 Hz, 2-NC_5H_4), 7.66 (1H, dt, ^3J = 4.7 Hz, ^3J = 9.0 Hz, 4-NC_5H_4), 7.46 (4H, d, ^3J = 7.9 Hz, 2-C_6H_4Me), 7.12 (6H, d, ^3J = 7.9 Hz, overlapping 3-C_6H_4Me, 3- and 5-NC_5H_4), 5.32 (1H, sept., ^3J = 6.1 Hz, $OCHMe_2$ *cis* to py), 5.16 (1H, sept., ^3J = 6.1 Hz, $OCHMe_2$ *trans* to py), 3.94 (2H, s, $pyCH_2N$), 3.40 (4H, m, $TsNCH_2CH_2N$), 3.10 (2H, m, $TsNCH_2CH_2N$), 2.88 (2H, m, $TsNCH_2CH_2N$), 2.35 (6H, s, C_6H_4Me), 1.51 (6H, d, ^3J = 6.1 Hz, $OCHMe_2$ *cis* to py), 1.37 (6H, d, ^3J = 6.1 Hz, $OCHMe_2$ *trans* to py) ppm. ^{13}C-{^{1}H} NMR (CD_2Cl_2, 75.4 MHz): δ 158.8 (6-NC_5H_4), 152.2 (2-NC_5H_4), 143.4 (1-C_6H_4Me), 143.2 (4-C_6H_4Me), 140 (3-NC_5H_4), 131.4 (3-C_6H_4Me), 128.1 (2-C_6H_4Me), 125.6 (4-NC_5H_4), 121.6 (5-NC_5H_4), 85.4 ($OCHMe_2$ *cis* to py), 81.7 ($OCHMe_2$ *trans* to py), 62.9 ($pyCH_2N$), 61.8 ($TsNCH_2CH_2N$), 50.9 ($TsNCH_2CH_2N$), 28.6 ($OCHMe_2$ *cis* to py), 28.3 ($OCHMe_2$ *trans* to py), 23.4 (C_6H_4Me) ppm. IR: 3435 (w), 1607 (s), 1290 (m), 1280 (m), 1141 (s), 1088 (s), 1018 (s), 969 (m), 942 (m), 920 (m), 854.5 (w), 832 (m), 774 (w), 665 (m), 600 (m), 554 (m), 508 (m) cm^{-1}. Anal. found (calcd. for $C_{30}H_{42}N_4O_6S_2Ti$); C, 54.05 (54.05); H, 6.45 (6.35); N, 8.28 (8.40) %.

Alternative NMR Tube Scale Synthesis of $Ti(L^{py})(O^iPr)_2$ (12). To a solution of $Ti(NMe_2)_2(O^iPr)_2$ (6.1 mg, 23.8 μmol) in CD_2Cl_2 (0.2 mL) was added a solution of H_2L^{py} (12 mg, 23.8 μmol) in CD_2Cl_2 (0.2 mL). A color change of the initially light brown to light yellow was observed. After 1 h analysis by ^{1}H NMR indicated that **12** had been formed quantitatively.

$Zr(L^{py})(O^iPr)_2$ (13). A slurry of H_2L^{py} (1.00 g, 2.00 mmol) in toluene (50 mL) was added to a solution of $Zr(O^iPr)_4 \cdot HO^iPr$ (3.00 g, 7.80 mmol) in toluene (20 mL). The mixture was heated at 100 °C for 16 h, resulting in an off-white slurry. The solid was filtered off and washed with pentane (3 × 30 mL). Recrystallization from a saturated benzene solution layered with hexanes yielded **13** as a white solid that was washed with pentane (3 × 20 mL) and dried in vacuo. Yield: 0.60 g (42%). ^{1}H NMR (C_6D_6, 299.9 MHz, 343 K): δ 9.47 (1H, br. m, 2-NC_5H_4), 8.25 (4H, br. d, ^3J = 6.0 Hz, 2-C_6H_4Me), 6.95 (5H, br. d, ^3J = 6.0 Hz, overlapping 3-C_6H_4Me and 4-NC_5H_4), 6.68 (1H, br. m, 3-NC_5H_4), 6.42 (1H, br. d, ^3J = 6.1 Hz, 5-NC_5H_4), 5.16 (1H, br. sept, ^3J = 6.0 Hz, $OCHMe_2$ *cis* to py), 4.62 (1H, br. sept, ^3J = 6.1 Hz, $OCHMe_2$ *trans* to py), 3.62 (2H, br. s, $pyCH_2$), 3.17, (4H, br. m, $TsNCH_2CH_2$), 2.54 (4H, $TsNCH_2CH_2$), 1.97 (6H, s, C_6H_4Me), 1.58 (6H, br. d, ^3J = 6.1 Hz, $CHMe_2$ *cis* to py), 1.20 (6H, br. d, ^3J = 6.1 Hz, $CHMe_2$ *trans* to py). A satisfactory ^{13}C NMR spectrum could not be obtained because of the fluxional nature of the compound. IR: 3431 (w), 1605 (w), 1164 (m), 1016 (m), 961 (w), 815 (m), 723 (w), 666 (m), 557 (w) cm^{-1}. Anal. found (calcd. for $C_{30}H_{42}N_4O_6S_2Zr$); C, 50.85 (50.75); H, 5.92 (5.96); N, 7.89 (7.89) %.

$Ti(L^{OMe})(O^iPr)_2$ (14). A mixture of H_2L^{OMe} (0.15 g, 0.32 mmol) and $Ti(O^iPr)_4$ (2.0 mL, 6.76 mmol) was heated and stirred at 130 °C under dynamic vacuum (70 mbar) for 4 h. The mixture was cooled to RT resulting in a yellow solid which was recrystallized from saturated dichloromethane solution layered with pentane to yield **14** as a yellow solid that was washed with pentane (3 × 20 mL) dried in vacuo. Yield: 0.10 g (47%). ^{1}H NMR (CD_2Cl_2, 299.9 MHz): δ 7.74 (4H, d, ^3J = 9.0 Hz, 2-C_6H_4Me), 7.25 (4H, d, ^3J = 9.0 Hz, 3-C_6H_4Me), 5.16 (1H, sept., ^3J = 6.5 Hz, $OCHMe_2$ *cis* to OMe), 4.93 (1H, sept., ^2J = 6.5 Hz, $OCHMe_2$ *trans* to OMe), 3.91 (3H, s, OMe), 3.80 (2H, t, ^3J = 6.5 Hz, $MeOCH_2$), 3.42−3.12 (6H, m, overlapping $TsNCH_2$ and $TsNCH_2CH_2$), 2.74 (4H, m, overlapping $MeOCH_2CH_2$ and $TsNCH_2CH_2$), 2.37 (6H, s, C_6H_4Me), 1.41 (4H, d, ^3J = 6.5 Hz, $OCHMe_2$ *cis* to OMe), 1.14 (4H, d, ^3J = 6.5 Hz, $OCHMe_2$ *trans* to OMe) ppm. ^{13}C-{^{1}H} NMR (CD_2Cl_2, 75.4 MHz) δ 141.6 (1-C_6H_4Me), 141.5 (4-C_6H_4Me), 129.4 (3-C_6H_4Me), 127.3 (2-C_6H_4Me), 84.5 ($OCHMe_2$ *cis* to OMe), 81.5 ($OCHMe_2$ *trans* to OMe), 71.6 ($MeOCH_2$), 63.9 (OMe), 58.1 ($TsNCH_2$), 54.6 ($MeOCH_2CH_2$), 48.7 ($TsNCH_2CH_2$), 26.1 ($OCHMe_2$ *trans* to OMe), 25.9 ($OCHMe_2$ *cis* to OMe), 21.6 (C_6H_4Me) ppm. IR: 3428 (w), 1297 (m), 1284 (s), 1145 (s), 1090 (s), 959 (m), 855 (m), 829 (s), 758 (w), 602 (m), 506 (w) cm^{-1}. Anal. found (calcd. for $C_{27}H_{43}N_3O_7S_2Ti$); C, 51.08 (51.18); H, 6.88 (6.84); N, 6.61 (6.63) %.

Alternative Synthesis of $Ti(L^{OMe})(O^iPr)_2$ (14). A solution of H_2L^{OMe} (0.50 g, 1.1 mmol) in dichloromethane (30 mL) was added to a solution of $Ti(NMe_2)_2(O^iPr)_2$ (0.30 g, 1.2 mmol) in

(87) Bradley, D. C.; Thomas, I. M. *J. Chem. Soc.* **1960**, 3857.
(88) Diamond, G. M.; Jordan, R. F.; Petersen, J. L. *Organometallics* **1996**, *15*, 4030–4037.
(89) Benzing, E.; Kornicker, W. *Chem. Ber.* **1961**, 2263–2267.
(90) Kempe, R.; Arndt, P. *Inorg. Chem.* **1996**, *35*, 2644–2649.

Table 10. X-ray Data Collection and Processing Parameters for H_2L^{OMe} (**9**), $Ti(L^{py})(NMe_2)_2$ (**10**), $Ti(L^{OMe})(NMe_2)_2 \cdot 2(C_6H_6)$ (**11·2(C$_6$H$_6$)**), $Ti(L^{py})(O^iPr)_2$ (**12**), $Ti(L^{OMe})(O^iPr)_2$ (**14**), $Zr(L^{py})(O^iPr)_2$ (**13**), and $Zr(L^{OMe})(O^iPr)_2$ (**15**)

	9	**10**	**11·2(C$_6$H$_6$)**	**12**
empirical formula	$C_{21}H_{31}N_3O_5S_2$	$C_{28}H_{40}N_6O_4S_2Ti$	$C_{25}H_{41}N_5O_5S_2Ti \cdot 2(C_6H_6)$	$C_{30}H_{42}N_4O_6S_2Ti$
fw	469.63	636.70	759.89	666.70
temp/K	150	150	150	150
wavelength/Å	0.71073	0.71073	0.71073	0.71073
space group	$P\,2_12_12_1$	$P2_1/c$	$C2/c$	$P2_1/c$
a/Å	7.34540(10)	9.7433(3)	13.9610(5)	8.9177(18)
b/Å	13.02980(10)	18.4302(5)	12.7787(5)	9.6354(19)
c/Å	24.3794(3)	17.1845(5)	21.6251(10)	36.811(7)
α/deg	90	90	90	90
β/deg	90	90.163(1)	93.0481(12)	90.00(3)
γ/deg	90	90	90	90
V/Å^3	2333.33(5)	3085.8(2)	3852.5(3)	3163.0(11)
Z	4	4	4	4
d (calcd)/Mg·m^{-3}	1.337	1.370	1.310	1.400
abs coeff/mm^{-1}	0.265	0.456	0.378	0.451
R indices:[a]				
R_1 =	0.0298[b]	0.0380[b]	0.0672[b]	0.0788[c]
R_w =	0.0341[b]	0.0379[b]	0.0670[b]	
wR_2 =				0.2026

	14	**13**	**15**
empirical formula	$C_{27}H_{43}N_3O_7S_2Ti$	$C_{30}H_{42}N_4O_6S_2Zr$	$C_{27}H_{43}N_3O_7S_2Zr$
fw	633.66	710.04	677.01
temp/K	150	150	150
wavelength/Å	0.71073	0.71073	0.71073
space group	$P2_1/c$	$P\bar{1}$	$P2_1/c$
a/Å	9.9927(1)	9.2206(2)	10.01950(10)
b/Å	9.6963(1)	9.6331(2)	9.89890(10)
c/Å	31.4855(4)	18.7269(5)	31.5596(4)
α/deg	90	85.4348(14)	90
β/deg	92.733(1)	78.1548(15)	92.7258(6)
γ/deg	90	84.6582(16)	90
V/Å^3	3047.23(6)	1617.76(7)	3126.60(6)
Z	4	2	4
d (calcd)/Mg·m^{-3}	1.381	1.458	1.438
abs coeff/mm^{-1}	0.466	0.517	0.532
R indices:[a]			
R_1 =	0.0400[c]	0.0326[b]	0.0376[b]
R_w =		0.0370[b]	0.0355[b]
wR_2 =	0.0980[d]		

[a] $R1 = \sum||F_o| - |F_c||/\sum|F_o|$; $Rw = \sqrt{\{\sum w(|F_o| - |F_c|)^2/\sum w|F_o|^2\}}$; $wR2 = \sqrt{\{\sum w(F_o^2 - F_c^2)^2/\sum w(F_o^2)^2\}}$. [b] For data with $I > 3\sigma(I)$. [c] For data with $I > 2\sigma(I)$. [d] For all data.

dichloromethane (30 mL). The mixture was stirred for 2 h, resulting in a yellow solution. Removal of the volatiles under reduced pressure afforded a yellow solid that was recrystallized from a concentrated dichloromethane solution layered with pentane to give **14** as a yellow solid that was washed with pentane (3 × 20 mL) and dried in vacuo. Yield: 0.52 g (78%).

Zr(L^{OMe})(O^{i}Pr)$_2$ (15). A mixture of H_2L^{OMe} (0.11 g, 0.23 mmol) and $Zr(O^iPr)_4 \cdot HO^iPr$ (0.50 g, 1.29 mmol) was heated with stirring at 125 °C under dynamic vacuum (75 mbar) for 5 h. The mixture was cooled to RT resulting in a yellow solid which was crystallized from saturated dichloromethane solution layered with pentane to yield **15** as a pale yellow solid that was washed with pentane (3 × 20 mL) and dried in vacuo. Yield: 0.07 g (41%). ^{1}H NMR (CD_2Cl_2, 499.9 MHz, 273 K): δ 7.82 (4H, br. d, ^3J = 7.0 Hz, 2-SC$_6$H$_4$), 7.26 (4H, br. d, ^3J = 7.0 Hz, 3-SC$_6$H$_4$), 4.52 (1H, br. sept. ^3J = 5.8 Hz, OC<u>H</u>Me$_2$ *cis* to OMe), 4.41 (1H, br. sept. ^3J = 5.8 Hz, OC<u>H</u>Me$_2$ *trans* to OMe), 3.93 (2H, s, C<u>H$_2$</u>py), 3.24−2.81 (8H, br. m), 2.37 (6H, s, C$_6$H$_4$<u>Me</u>), 1.21 (6H, br. d, ^3J = 6.1 Hz, OCH<u>Me$_2$</u> *cis* to OMe), 1.11 (6H, br. d, ^3J = 6.0 Hz, OCH<u>Me$_2$</u> *trans* to OMe). A satisfactory ^{13}C NMR spectrum could not be obtained because of the fluxional nature of the compound. IR: 3453 (w), 1599 (w), 1299 (m), 1143 (w), 1105 (m), 1060 (m), 1024. (w), 962 (w), 939 (m), 829 (w), 669 (w) cm^{-1}. cm^{-1}. Anal. found (calcd. for $C_{27}H_{43}N_3O_7S_2Zr$); C, 47.87 (47.90); H, 6.31 (6.40); N, 6.17 (6.21) %.

Crystal Structure Determinations of H$_2$L^{OMe} (9), Ti(L^{py})(NMe$_2$)$_2$ (10), $Ti(L^{OMe})(NMe_2)_2$ (11), $Ti(L^{py})(O^iPr)_2$ (12), $Zr(L^{py})(O^iPr)_2$ (13), $Ti(L^{OMe})(O^iPr)_2$ (14), and $Zr(L^{OMe})(O^iPr)_2$ (15). Crystal data collection and processing parameters are given in Table 10. Crystals were mounted on glass fibers using perfluoropolyether oil and cooled rapidly in a stream of cold N_2 using an Oxford Cryosystems Cryostream unit. Diffraction data were measured using an Enraf-Nonius KappaCCD diffractometer. As appropriate, absorption and decay corrections were applied to the data and equivalent reflections merged.[91] The structures were solved with SIR92[92] or SHELXS-97[93] and further refinements and all other crystallographic calculations were performed using either the CRYSTALS program suite[94] or SHELXS-97.[95] Other

(91) Otwinowski, Z.; Minor, W. *Processing of X-ray Diffraction Data Collected in Oscillation Mode*; Academic Press: New York, 1997.
(92) Altomare, A.; Cascarano, G.; Giacovazzo, G.; Guagliardi, A.; Burla, M. C.; Polidori, G.; Camalli, M. *J. Appl. Crystallogr.* **1994**, *27*, 435.
(93) Sheldrick, G. M. *Acta Crystallogr., Sect. A* **1990**, *46*, 467.
(94) Betteridge, P. W.; Cooper, J. R.; Cooper, R. I.; Prout, K.; Watkin, D. J. *J. Appl. Crystallogr.* **2003**, *36*, 1487.
(95) Sheldrick, G. M.; Schneider, T. R. *Methods Enzymol.* **1997**, *277*, 319–343.

details of the structure solution and refinements are given in the Supporting Information (CIF data). A full listing of atomic coordinates, bond lengths and angles and displacement parameters for all the structures have been deposited at the Cambridge Crystallographic Data Centre. See Notice to Authors, Issue No. 1.

General Procedure for Polymerization of ε-CL. Parallel duplicate experiments were carried out in each of which a solution of ε-CL (6.6 mmol) in toluene (3.0 mL) was heated to 100 °C and added to a solution of catalyst (0.066 mmol) in toluene (3.8 mL) also at 100 °C. For one sample aliquots were taken at the respective time. Upon completion the reaction was quenched by addition of wet THF (10 mL), and the solution evaporated to dryness to give the crude polymer. Isolated yields were obtained from the parallel experiment for which the polymer was quenched by wet THF (10 mL) and precipitated by addition to ethanol (250 mL) with vigorous stirring, filtered and dried to constant weight in vacuo.

General Procedure for Solution Polymerization of *rac*-LA. *rac*-LA (6.00 mmol) and catalyst (0.06 mmol) were added to a Schlenk flask and heated to 70 °C. To this, hot (70 °C) toluene (6.0 mL) was added, rapidly disolving both solids. The resultant solution was heated at 70 °C, and aliquots were taken at the respective time. Upon completion of the reaction wet THF (10 mL) was added, and the solution evaporated to dryness to give the poly(*rac*-LA). Conversions were determined by ^{1}H NMR integration of the OC<u>H</u>Me resonance relative intensities of the residual *rac*-LA and po<u>l</u>y(*rac*-LA).

General Procedure for Solventless (Melt) Polymerization of *rac*-LA. A Schlenk flask was charged with catalyst and *rac*-LA at the desired ratio and heated at 130 °C for 30 min with stirring. The mixture was cooled to RT, and wet THF (10 mL) was then added and the resulting solution evaporated to dryness to give the crude polymer.

Acknowledgment. We thank the EPSRC for support.

Supporting Information Available: X-ray crystallographic data in CIF format for the structure determinations of **9**−**15**; additional data concerning the ROP catalysis. This material is available free of charge via the Internet at http://pubs.acs.org.